The role of climate change in drainage network reorganization: insights from numerical experiments

Emanuele Giachetta(1) *, Nicole M. Gasparini(2), Domenico Capolongo(1), Alberto Refice(3), and Frank J. Pazzaglia(4).

(1) *Dipartimento di Geologia e Geofisica, Università degli studi di Bari, Italy* (egiachetta@uniroma3.it),
(2) *Department of Earth and Environmental Sciences, Tulane University, USA* (ngaspari@tulane.edu),
(3) *Istituto di Studi sui Sistemi Intelligenti per l'Automazione, Consiglio Nazionale delle Ricerche (ISSIA-CNR), Bari, Italy* (refice@ba.issia.cnr.it),
(4) *Department of Earth and Environmental Sciences, Lehigh University, USA* (fjp3@lehigh.edu)
* now at *Laboratory of Experimental Tectonics, Dipartimento di Scienze Geologiche, Università degli Studi Roma Tre, Italy*

ABSTRACT

The continuous feedbacks among tectonics, surface processes, and climate change are reflected in the distribution of catchments on active mountain fronts.
Previous studies (e.g. Hovius, 1996) have shown a certain regularity of valley spacing on several mountain ranges worldwide, but what is at the origin of such geomorphological feature of landscapes is currently not well known.
In this work, we illustrate numerical experiments of long-term landscape evolution of an active mountain range.
We show how the constant valley spacing, achieved at steady state on both sides of the range, is progressively restored after simulating a migration of the main drainage divide caused by a precipitation gradient applied across the mountain belt.
We analyze the time evolution of the spacing ratio R (Hovius,1996; Wallace, 1978), defined as the ratio between the half-width W of the belt and the spacing S of the outlets of the catchments draining from the main drainage divide.
We consider R as an index describing the degree of catchment reorganization on both the windward and leeward sides of the belt.

THEORY

A number of studies have quantitatively described the phenomenon using the valley spacing ratio (see Fig. 1A):

$$R = W/\lambda, \quad (1)$$

where W represents the distance from the main divide to the mountain front, while λ is the distance between outlets along the mountain front (Hovius, 1996). Numerical studies have focused on spatial scales both across mountain ranges and within single watersheds. Perron et al. (2009) showed that first-order valley spacing can be predicted by calculating a characteristic length scale at which erosion rates from hillslope diffusion and river incision are equal. They also showed that the charachteristic length is proportional to a quantity similar to a Peclét number Pe, calculated from the numerical model parameters and the surface states, and given by:

$$\mathrm{Pe} = k_c \cdot \ell^{\,2(m+1)-n} / k_d\, \zeta^{\,1-n} \quad (2)$$

(see model section for parameters description). Furthermore, using numerical experiments and data from real field sites, Perron et al. (2009) demonstrated that valley spacing within watersheds is directly linked to valley spacing at mountain front.
Previous experimental observation of regular valley spacing at larger spatial scales has been partially addressed with numerical modeling studies (e.g. Ellis et al., 1999), and numerical experiments using coupled tectonic and geomorphological

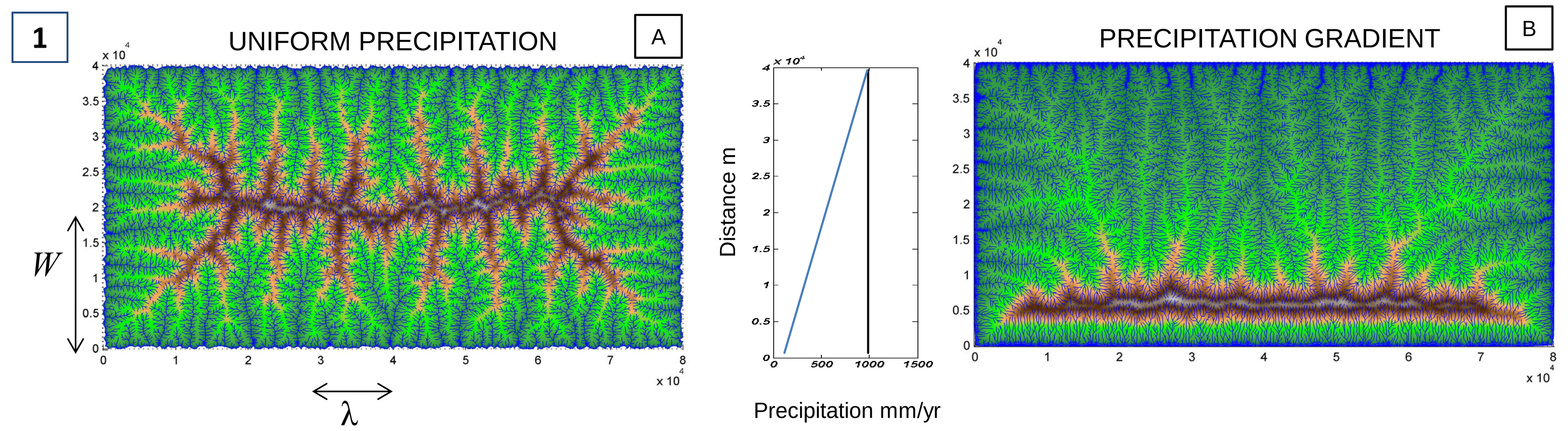

EXPERIMENTAL SETTINGS

We simulate landscapes of various sizes, with a fixed TIN mean sampling distance of 100 m; the initial surface is completely flat at zero elevation. Sediment can flow across all four landscape boundaries.

We apply a spatially uniform and constant uplift rate of 1 mm/y over the whole domain. The surface processes and tectonic models are run with variable time steps (to preserve numerical stability in the finite-volume approximation used to solve eq. 3).

After the initial topography has reached a steady state under a uniform, constant precipitation rate of 1 m/y, a precipitation gradient is introduced, in a direction perpendicular to the belt axis, to simulate "orographic" precipitation; the maximum precipitation rate is maintained at 1 m/y along the upper side, and it linearly decreases towards the opposite side reaching a minimum of 0.2 m/y (see plot of precipitation across the belt in Fig. 1).

We calculate the mean spacing ratio R of the main fluvial valleys and observe the evolution of the simulated catchments through time.

In Fig. 2, a 3D plot of calculated values of $\lambda' = 1/R$, and Pe vs. time is shown for three simulated landscapes of different size: 4 km x 2 km, 6 km x 3 km and 8 km x 4 km.

Figs. 4-5-6 represent respectively the time evolution of λ', the normalized relief ζ, and Pe, either for the wet side (blue line) and the dry side (red line) of the simulated surface of size 8 km x 4 km.

THE MODEL

SIGNUM includes simulation of diffusive and advective erosion processes, tectonic uplift, and climate changes modeled as a change from uniform precipitation to a precipitation gradient. Changes in elevation of the topographic surface are described by the equation of mass conservation, (e.g., Tucker et al., 2001a):

$$\frac{\partial z}{\partial t} = U - k_c Q^m (\nabla z)^n - \nabla q_s \quad (3)$$

where z is the elevation of a point on the TIN, t is time and U is tectonic uplift. The second term on the right-hand side represents the stream power law for fluvial incision model. The water discharge term Q is often approximated by the expression $Q = \sum P_i \cdot a_i$, where P_i is the local mean annual precipitation rate and a_i is the area for a given upstream point at location i (Roe et al., 2002). The last term in the right-hand side represents erosion from hillslope processes. In the experiments shown here, we use the linear diffusion equation for hillslope sediment flux q_s:

$$q_s = k_d \nabla z$$

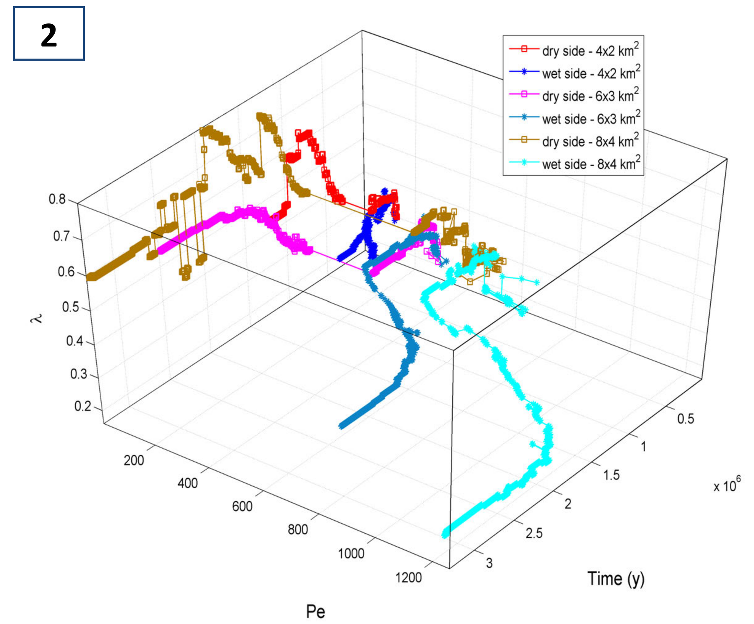

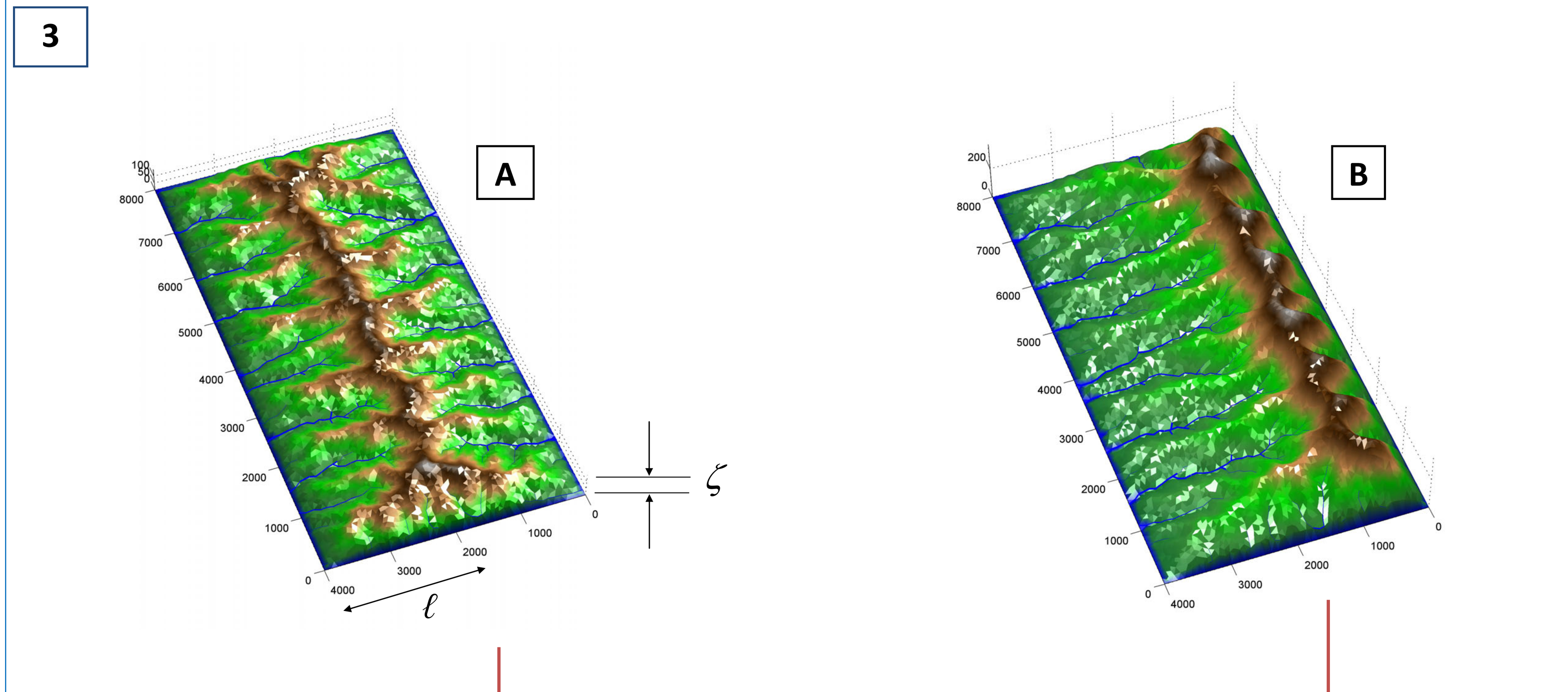

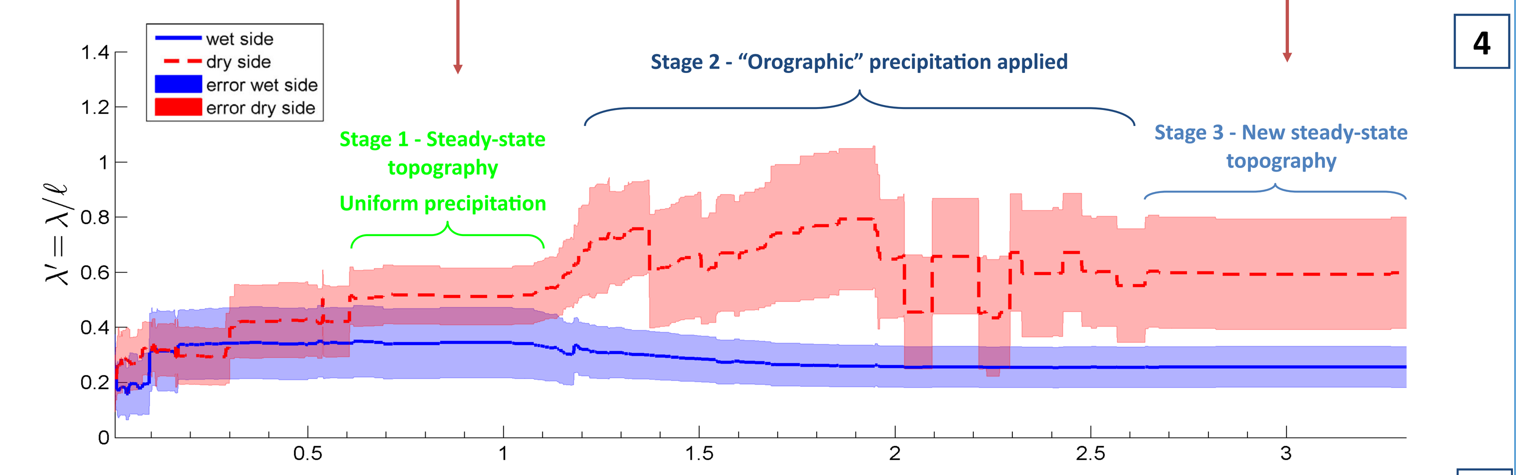

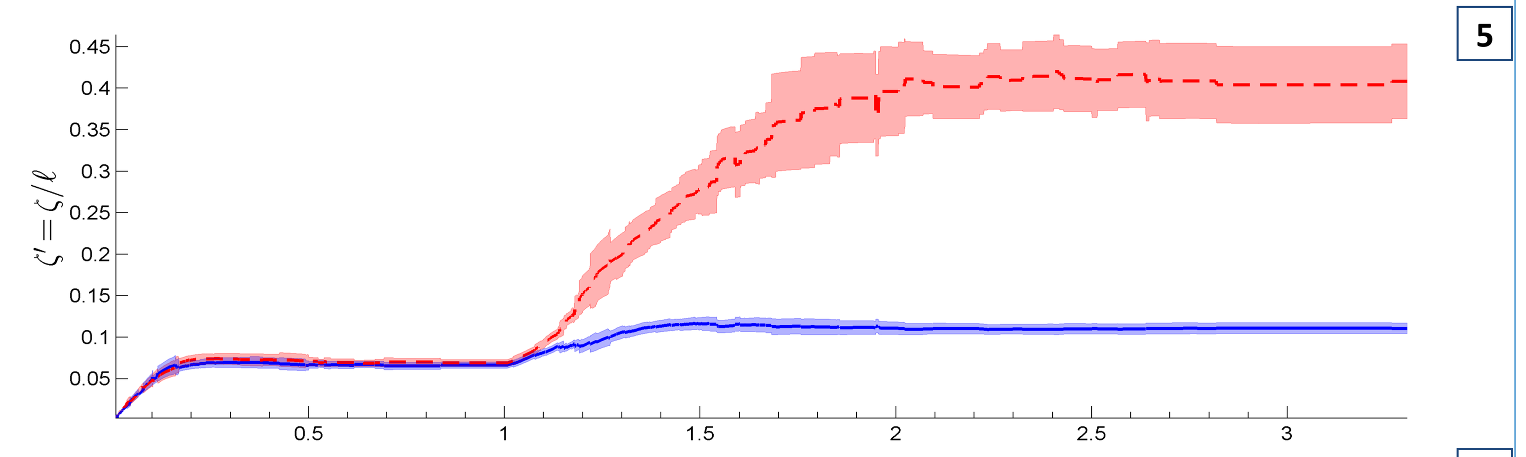

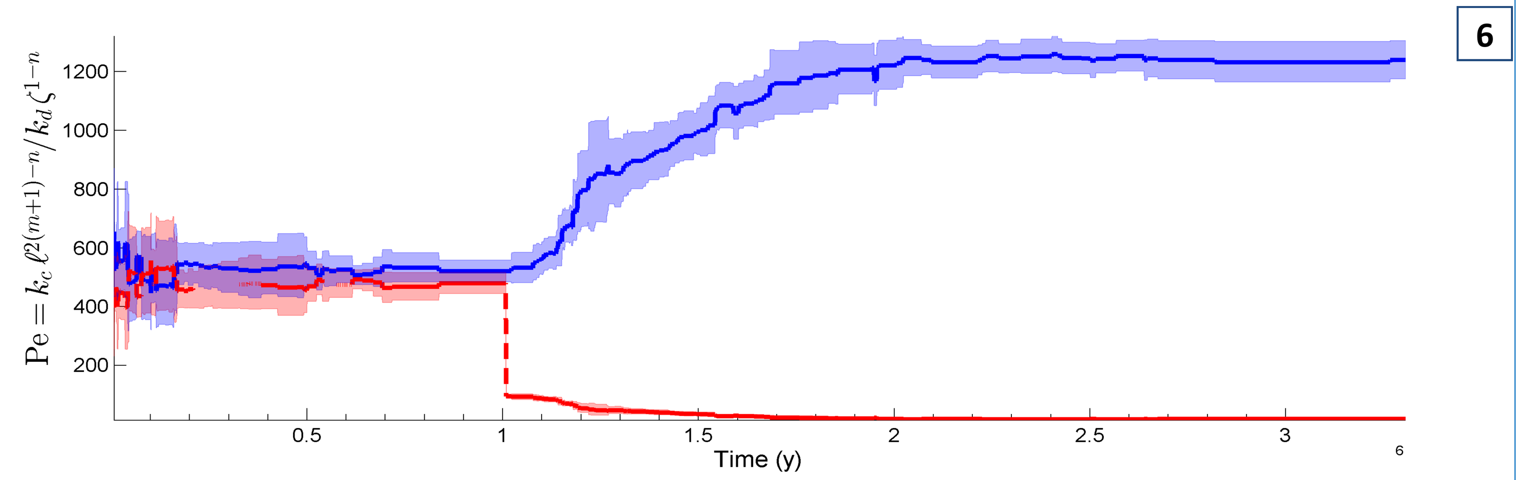

TEMPORAL EVOLUTION ANALYSIS

Evolution stage 1: in Fig. 3A, the landscape has reached the steady-state topography under uniform precipitation. The pattern of catchments, illustrated in Fig. 7, consists of an alternation of larger, and smaller catchments etched on the triangular facets.

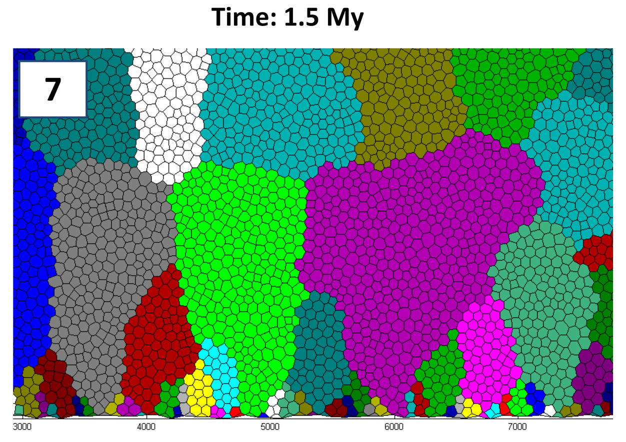

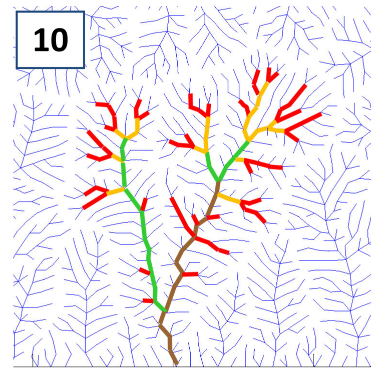

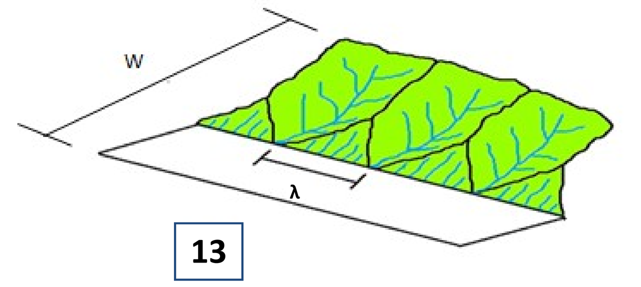

Evolution stage 2: after the precipitation gradient is applied, the main divide of the belt is pushed from the wet side towards the dry side, where larger catchments shrink and, simultaneously, the smaller catchments on triangular facets grow (Fig. 8).

Furthermore, the drainage network and maximum stream order is consequently reduced in the larger watersheds and viceversa for the smaller watersheds (see sequence of Figs. 10-11-12).

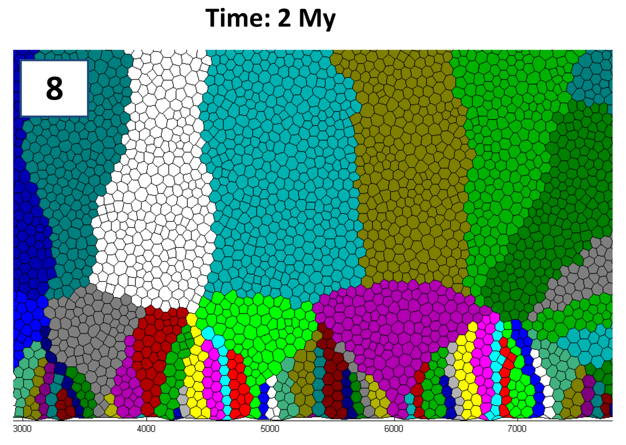

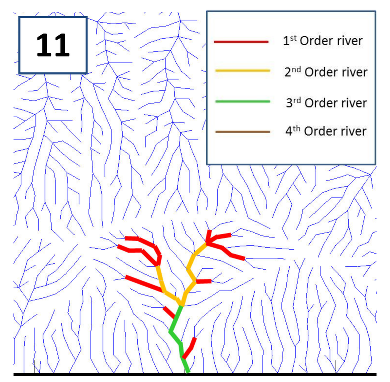

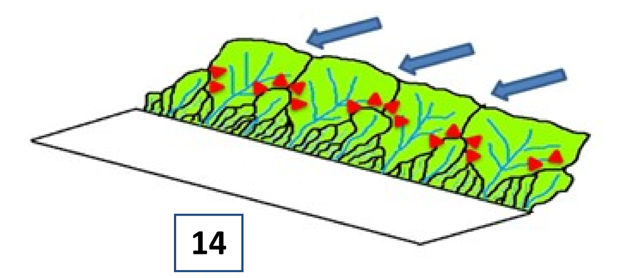

Evolution stage 3: a new steady state topography is reached under changed climatic conditions (Fig. 3B); on the dry side of the belt, the spacing ratio R is maintained (see plot of $\lambda' = 1/R$ vs Time in Fig. 4) through catchment reorganization (sequence illustrated in the sketch of Figs. 13-14-15). In the final stage of landscape evolution, a "normalization" of the pattern of watersheds can be also observed (Fig. 9).

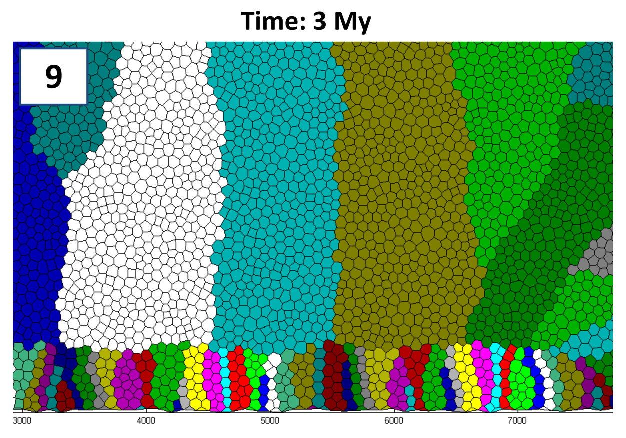

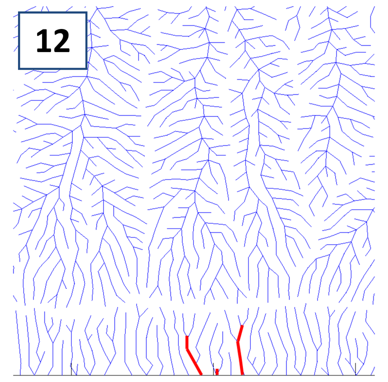

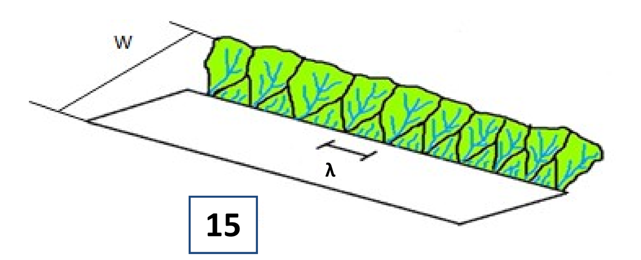

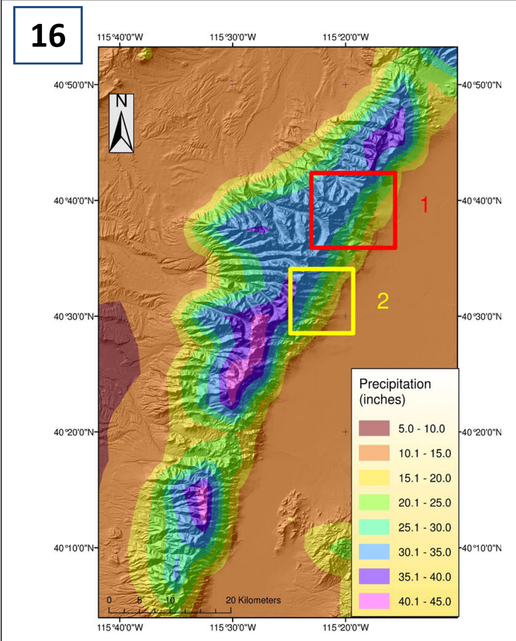

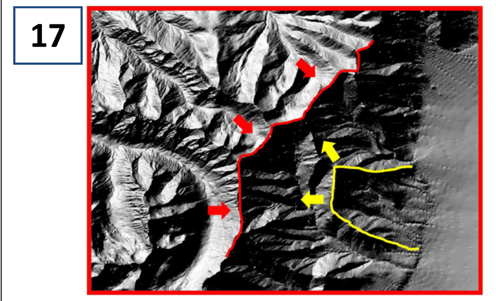

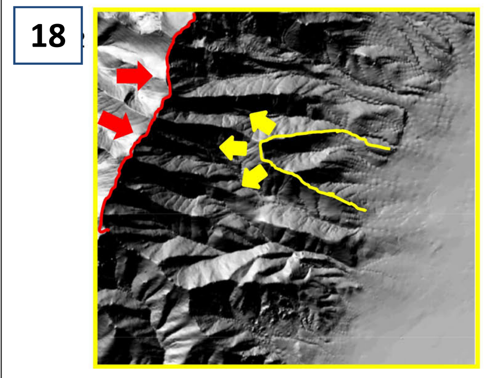

REAL DATA COMPARISON

A real-world example of the behavior corresponding to the simulated numerical results described above can be seen along the Ruby Mountains, as suggested by Ellis et al. (1999).
In the Basin and Range area, the air circulation is mainly from West to East. When moist air from the Pacific Ocean encounters a topographic barrier such as the Ruby Mountains, it is forced to move upward and over the obstacle, losing moisture in form of heavy precipitation on the western flank. This also results in a lack of precipitation on the eastern side of the range.
A PRISM (Daly et al., 1994) average annual precipitation map of the area from the period 1961-1990 is shown in Fig. 16. The Ruby Mountains are an uplifted core complex, bounded by active normal faults and there are enough similarities to warrant comparison with our numerical modeling results.
We know that the drainage basins emphasized here have been significantly impacted by geomorphic processes neglected in the numerical model (glaciation and cirque headwall processes that accompany alpine glaciations).
In fact, the rivers that currently drain the Ruby Mountains are largely out of equilibrium with respect to their long profiles and sediment transport, because they have inherited valleys significantly modified by recent glaciations.
Nevertheless, some analogies between the transient topography in the numerical model simulation and on the leeward side of the Ruby range are highlighted in Figs. 17 and 18. In particular, potential examples of the main drainage divide migration, the shrinking of the larger catchments and the growth of triangular facets, which look similar to the simulated basins in our numerical experiments, are highlighted.

INTERPRETATION

Valley spacing appears to be set by the interplay among river incision and hillslope processes, which are driven by tectonic and climate forcings.
The numerical results show that change in the precipitation pattern can exert a strong control on drainage network development and reorganization on both sides of the simulated mountain belt. In particular, the leeward side shows a more interesting evolution, because the interaction amongst all geomorphic processes leads to a significant catchment reorganization.
The final result of this complex mechanism of watershed reorganization is a new steady state topography, at which the mean spacing ratio on either sides of the range has almost the same value (within +/− 15%) as the former steady state with uniform precipitation (see plot of λ' vs. time in Fig. 4).
Furthermore, the model of watersheds development proposed here, can explain some real landscapes in which we found analogies with the different evolutionary stages of the simulated belts.

References

Bonnet, S. (2009). Shrinking and splitting of drainage basins in orogenic landscapes from the migration of the main drainage divide, *Nature Geoscience*, 2, 766-771.

Capolongo, D., Refice, A., and Giachetta, E (2011). Investigating valley spacing dynamics in linear mountain fronts through terrain numerical modeling, *EGU Abstracts*.

Daly, C., Neilson, R.P., and Phillips, D.L. (1994). A statistical-topographic model for mapping climatological precipitation over mountainous terrain. *Journal of Applied Meteorology*, v. 33, 140–158.

Ellis, M., Densmore, A.L., and Anderson, R.S. (1999). Development of mountainous topography in the Basin Ranges, USA, *Basin Research*, v. 11, p. 21–41.

Hovius, N. (1996), Regular spacing of drainage outlets from linear mountain belts, *Basin Research*, 8, 29-44.

Perron, J.T., Kirchner, J.W., and Dietrich, W.E. (2009). Formation of evenly spaced ridges and valleys, *Nature* 460, 502-505.

PRISM Climate Group (2006), Oregon State University: http://prism.oregonstate.edu.

Refice, A. Giachetta, E., Capolongo, D. (2012). SIGNUM: a Matlab, TIN-based landscape evolution model, *Computers & Geosciences*, in press.

Tucker, G.E., Lancaster, S.T., Gasparini, N.M., Bras, R.L. and Rybarczyk, S.M. (2001). An Object-oriented Framework for Distributed Hydrologic and Geomorphic Modeling using Triangulated Irregular Networks. *Computers & Geosciences*. 27: 959-973.

Wallace, R.E. (1978). Geometry and rate of changes of fault-generated range fronts, northcentral Nevada. *Jour. Research U.S. Geol. Survey*, 6, 637-650.